Rothamsted Repository Download

A - Papers appearing in refereed journals

Shewry, P. R., Wan, Y., Hawkesford, M. J. and Tosi, P. 2019. Spatial distribution of functional components in the starchy endosperm of wheat grains. *Journal of Cereal Science.* 91 (January), p. 102869.

The publisher's version can be accessed at:

- https://dx.doi.org/10.1016/j.jcs.2019.102869

The output can be accessed at: https://repository.rothamsted.ac.uk/item/96yz0/spatial-distribution-of-functional-components-in-the-starchy-endosperm-of-wheat-grains.

13/12/2019 09:49   repository.rothamsted.ac.uk   library@rothamsted.ac.uk

Journal Pre-proof

Spatial distribution of functional components in the starchy endosperm of wheat grains

Peter R. Shewry, Yongfang Wan, Malcolm J. Hawkesford, Paola Tosi
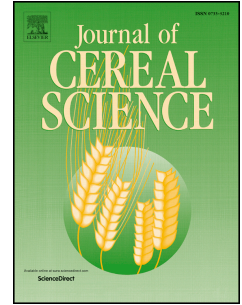
Please cite this article as: Shewry, P.R., Wan, Y., Hawkesford, M.J., Tosi, P., Spatial distribution of functional components in the starchy endosperm of wheat grains, *Journal of Cereal Science* (2019), doi: https://doi.org/10.1016/j.jcs.2019.102869.

This is a PDF file of an article that has undergone enhancements after acceptance, such as the addition of a cover page and metadata, and formatting for readability, but it is not yet the definitive version of record. This version will undergo additional copyediting, typesetting and review before it is published in its final form, but we are providing this version to give early visibility of the article. Please note that, during the production process, errors may be discovered which could affect the content, and all legal disclaimers that apply to the journal pertain.
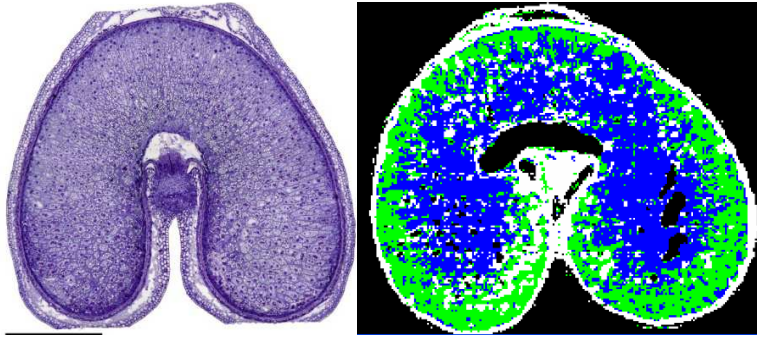
Radial gradients in composition in developing grain of wheat: left, section stained to show protein and starch (left) and right, pattern of arabinose substitution of cell wall arabinoxylan revealed by FT-IR microspectroscopy

1   Spatial distribution of functional components in the starchy endosperm of wheat grains

2   Peter R Shewry[a*], Yongfang Wan[a], Malcolm J Hawkesford[a] and Paola Tosi[b].

3   [a]Plant Science Department, Rothamsted Research, Harpenden, Herts, AL5 2JQ, UK.

4   [b]School of Agriculture, Policy and Development, University of Reading, Whiteknights

5   Campus, Early gate RG6 6AR, Reading UK

6

7   *Corresponding author.

8   Email addresses: peter.shewry@rothamsted.ac.uk; yongfang.wan@rothamsted.ac.uk;

9   malcolm.hawkesford@rothamsted.ac.uk; p.tosi@reading.ac.uk.

10

11   **Abstract**

12   The starchy endosperm of the mature wheat grain comprises three major cell types, namely

13   sub-aleurone cells, prismatic cells and central cells, which differ in their contents of

14   functional components: gluten proteins, starch, cell wall polysaccharides (dietary fibre) and

15   lipids. Gradients are established during grain development but may be modified during grain

16   maturation and are affected by plant nutrition, particularly nitrogen application, and

17   environmental factors. Although the molecular controls of their formation are unknown, the

18   high content of protein and low content of starch of sub-aleurone cells, compared to the

19   other starchy endosperm cells types, may result from differences in developmental

20   programming related to the cells having a separate origin (from anticlinal division of the

21   aleurone cells). The gradients within the grain may be reflected in differences in the

22   compositions of mill streams, particularly those streams enriched in the central and outer

23   cells of the starchy endosperm, respectively, allowing the production of specialist flours for

24   specific end uses.

25   **Key words: wheat, white flour; starchy endosperm; starch; lipids; gluten proteins;**

26   **polysaccharides; dietary fibre**

27   **Abbreviations**

28   A, arabinose; AX, arabinoxylan, AXOS, arabinoxylan oligosaccharide; DP, degree of

29   polymerisation; DPA, days past anthesis; FTIR, Fourier transform infrared; GL, galactolipid;

30   HMW, high molecular weight; LMW, low molecular weight; NMR, nuclear magnetic

31   resonance; TAG, triacylglycerol; PL, phospholipid; SIMS, secondary ion mass spectrometry;

32   TDF, total dietary fibre; WE, water-extractable; WU, water-unextractable; X, xylose

33

34

1. Introduction

36 Wheat is used for a wide range of foods, from globally consumed forms such as bread,
37 cakes, biscuits, pasta and noodles to regional and traditional foods such as couscous and
38 bulgar. As the mature wheat kernel is dry and hard it can only be consumed after
39 processing, which for most products starts with a form of milling. Milling fulfils two purposes:
40 to reduce the grain to flour and to separate the different grain tissues. This separation is
41 required because the grain has a complex structure, comprising several tissues which differ
42 in their compositions, functional properties, health benefits and palatability to consumers. For
43 most food applications milling is used to separate the starchy endosperm tissue of the grain
44 and reduce it to fine white flour. However, this coarse separation ignores the fine differences
45 in composition which exist both within and between tissues. We consider that this variation
46 can be exploited by innovative milling methods, to develop specialist flours for specific end
47 uses.

1.1. The wheat grain

49 The wheat grain is a single seeded fruit (caryopsis) in which the maternal fruit coat
50 (pericarp) and seed coat (testa) surround the zygotic embryo and endosperm (Bechtel et al.,
51 2009). These tissues can be further divided: the embryo comprises a single storage
52 cotyledon (the scutellum) and the embryonic axis (plumule, radicle and hypocotyl) while the
53 endosperm consists of starchy endosperm cells surrounded by a single layer of aleurone
54 cells. The major tissue in the mature grain is the starchy endosperm, which accounts for
55 about 83-84% of the dry weight. By contrast, the embryo accounts for about 3% of the dry
56 weight, the aleurone about 6.5% and the outer layers (pericarp and testa) about 7-8%
57 (Barron et al, 2007).

58 The starchy endosperm is the major storage tissue, storing both starch and protein, and is
59 the origin of white flour produced by milling. Millers aim to recover the highest possible
60 proportion of this tissue, often achieving white flour yields equivalent to 78-80% of the grain
61 dry weight. However, this process is based on the assumption that the endosperm is
62 essentially homogeneous in composition which is not the case.

63 In fact, studies of developing and mature grain show that the cells present in the starchy
64 endosperm differentiate into three major types (which are illustrated in Figure 1) (Evers and
65 Millar, 2002). Beneath the single layer of aleurone cells are two to three layers of protein-
66 rich sub-aleurone cells and beneath these are elongated prismatic cells which radiate
67 towards the centre of the grain (Figure 1, area B). Finally, the cells in the central parts of the

68   cheeks of the grain are round or polygonal and become highly extended with starch (Figure

69   1, area A). Bradbury et al (1956) reported approximate sizes of 60 μm diameter for the sub-

70   aleurone cells, 128-200 μm x 40-60 μm for the prismatic cells and 72-144 x 69-120 μm for

71   the central cells.

72   These differences in cell size and morphology are accompanied by differences in

73   composition, resulting in radial and longitudinal gradients.

74   *1.2.   Analysis of gradients by pearling and imaging.*

75   Two approaches have been taken to study gradients in developing and mature grain.

76   Sections of grain tissue can be analysed by various imaging approaches, ranging from

77   simple light microscopy of stained and fixed tissues with components visualised by staining

78   or immunochemistry, to sophisticated chemical imaging such as Fourier Transform Infrared

79   (FT-IR) microspectroscopy (Barron et al., 2005; Toole et al., 2009, 2010, 2011), Raman

80   microspectroscopy (Philippe et al, 2006; Toole et al., 2009), MALDI MSI (Fanuel et al.,

81   2018), and Secondary Ion Mass Spectrometry (NanoSIMS) (Moore et al., 2016). In general,

82   these approaches are more readily applied to developing tissues than to mature grain, due

83   to the ease of sectioning and the lower content of starch. Chemical imaging also requires

84   specialist equipment and is generally low throughput. For example, modern NanoSIMS

85   equipment costs in excess of £3m with a maximum throughput of about 1 sample a day.

86   Although it is possible to carry out biochemical and chemical analyses on material prepared

87   by hand-dissection of grain (for example, Saulnier et al, 2009), this approach is limited by the

88   amount of time required for preparation. A more widely used method is to remove sequential

89   fractions from the outside of the grain using pearling (as described for barley by Millet et al.,

90   1991 and for wheat by He et al., 2013). The application of pearling to wheat is illustrated in

91   Figure 2. Laboratory scale pearling mills, such as that shown in Figure 2, are generally used

92   for grain samples of about 50g, to generate fractions of between 3 to 5 g each. However,

93   these fractions do not correspond precisely to botanical tissues and pearling has two

94   important limitations. Firstly, because the grain is elongated the removal of tissue is not

95   even, with more removed from the end of the grain (which consequently becomes

96   progressively more rounded). Secondly, the tissue within the groove is not removed, with the

97   groove still being apparent when over 40% of the grain weight has been removed (Figure 2).

98   Nevertheless, the fractions still provide a broad view of the distribution of components within

99   the whole grain.

100   **2. Radial gradients in the starchy endosperm**

101   *2.1. Protein*

102 Differences in protein content and composition have been known for many years, with the
103 sub-aleurone cells being richer in protein and having fewer and less regular in shape starch
104 granules, compared with other starchy endosperm cells (Bradbury et al, 1956; Kent, 1966;
105 Kent and Evers, 1969). In fact, Kent (1966) calculated that the sub-aleurone cells in a flour of
106 12.5% protein contained 54% protein (whereas 8% would be more typical for the central
107 cells), and this protein enrichment of the sub-aleurone can be clearly seen when grain
108 sections are stained to show the distribution of protein and other components (Figure 1).

109 In addition, there are well established gradients in protein composition. The most detailed
110 study so far used sequential pearling to remove six fractions each corresponding, on
111 average, to about 8% of the grain weight (He et al., 2013). Comparison of these fractions
112 and the milled core (corresponding to about 50% of the grain weight) showed that although
113 the total protein content decreased from the outer layers to the centre of the grain, the
114 proportion of gluten proteins increased, from about 50-55% to about 75% of the total protein
115 in grain from plants grown with 100kg/ha of N-fertilizer. Analysis of protein fractions by SDS-
116 PAGE and western blotting with antibodies to gluten proteins shows that there are also
117 gradients in gluten protein composition, with the proportions of HMW subunits of glutenin
118 and γ-gliadins increasing toward the centre the grain and proportions of some ω-gliadins
119 and α-gliadins decreasing (Tosi et al., 2011; He et al, 2013). However, SDS-PAGE does not
120 clearly separate the LMW subunits of glutenin from γ-gliadins and α-gliadins. He et al. (2013)
121 therefore also determined the size distribution of gluten proteins extracted using SDS by SE-
122 HPLC (Morel et al., 2000). This showed clear increases, from the outside to the centre of the
123 grain, in the proportions of the HMW glutenin polymers (%F1) that are considered to
124 contribute to gluten elasticity (Shewry et al., 2003) and, to a lesser extent, in the lower
125 molecular weight glutenin polymers (%F2). These gradients were reflected in an increase in
126 the ratios of HMW:LMW polymers (%F1/%F2 ratio), and of glutenin (F1+F2) to gliadin (F3
127 comprising mainly ω-gliadins + F4 comprising α- and γ-gliadins). Both of these ratios have
128 been used as predictors of breadmaking quality.

129 Zhou et al. (2018) also reported analyses of pearling fractions, but removed 8 fractions, each
130 corresponding to about 10% of the grain weight, with the core representing only 20% of the
131 total. The results were broadly consistent with those of He et al. (2013), although they
132 determined glutenin macropolymers (GMP), rather than the size distribution of glutenin
133 polymers by SE-HPLC, and expressed the amounts of all proteins as % dry weight.

134   *2.2. Starch.*

135 Starch is a mixture of two glucose polymers: amylose, which consists of unbranched (1→4)
136 α-linked chains comprising up to several thousand glucose units, and amylopectin, which

137 may comprise over 100,000 glucose units and is highly branched with (1→6) α-linkages as

138 well as (1→4) α-linkages. The proportion of amylose in wheat starch generally ranges from

139 about 18% to 35%. Mature wheat grain contains two distinct populations of starch granule,

140 referred to as A-type and B-type. These populations differ in size and morphology, with A-

141 type being > 10 μm and lenticular in shape and B-type about <10 μm and spherical in shape

142 (Stone and Morel, 2009). These populations also differ in polymer composition and structure

143 (Shinde et at 2003), with B-type granules containing lower proportions of amylose than A-

144 type granules (Duffus and Murdoch, 1979; Shinde et al., 2003).

145 Microscopy of developing and mature grain shows clear differences in the distribution of

146 starch within the starchy endosperm cells, with only a few small granules being present in

147 the protein-rich sub-aleurone cells (Figure 1) (as also discussed by Tomlinson and Denyer,

148 2003). This distribution is consistent with the increases in the total starch and % amylose

149 reported in pearling fractions by Tosi et al. (2018) and Zhou et al. (2018).

150 More detailed studies were reported by Zhou et al. (2018), who classified the starch granules

151 into three types: A (diameter 22-28 μm), B (7.4-7.7 μm) and C (2.9-3.24 μm) and showed

152 small but statistically significant differences in their mean diameters between pearling

153 fractions.

154 Starch has a major impact on the processing properties of flours, and both Tosi et al. (2018)

155 and Zhou et al. (2018) reported gradients in the properties of the starch (onset temperature

156 of gelatinisation and pasting properties) present in pearling fractions. However, it should be

157 noted that these properties are likely to be affected by effects of milling, particularly on starch

158 damage, which may be greater using a pearling mill (up to 18% damaged starch being

159 reported by Tosi et al, 2018) than in roller milling (generally up to about 12%).

160 *2.3. Cell wall polysaccharides.*

161 Cell wall polysaccharides are the major source of dietary fibre in cereal products and hence

162 are important for human nutrition and health. Whole grain contains about 11.5-15.5% (mean

163 13.4%) total dietary fibre (TDF), including 5.53-7.42% (mean 6.49%) arabinoxylan (AX),

164 1.67-3.05% (mean 2.11%) cellulose and 0.51-0.96% (mean 0.73%) β-glucan (Andersson et

165 al., 2013). However, all of the cellulose and much of the AX and β-glucan are located in the

166 outer (bran) layers, and white flour contains only about 2-3% cell wall polysaccharides, with

167 AX (70%) and β-glucan (20%) being the dominant components. Analyses of pearling

168 fractions have shown that TDF, AX and β-glucan all decrease in concentration from the

169 outer to inner layers (Zhou et al., 2018; Tosi et al., 2018). However, a series of studies have

170 focused on variation in the fine structures of these components.

171 AX comprises a backbone of β-D-xylopyranosyl (xylose) residues linked through (1→4)
172 glycosidic linkages, with some residues being substituted with α-L-arabinofuranosyl
173 (arabinose) residues at either one or two positions. Some arabinose residues present as
174 single substitutions may be further substituted with ferulic acid at the 5-position, which may
175 form diferulate cross-links between polymers. AX is often divided into two classes,
176 depending on whether it is extractable (WE-AX) or unextractable (WU-AX) with water. β-
177 glucan comprises glucose residues joined by (1→3) and (1→4) linkages. Single (1→3)
178 linkages are usually separated by two or three (1→4) linkages, but longer stretches of up to
179 14 (1→4) linked glucan units (sometimes referred to as "cellulose-like" regions) have been
180 reported for wheat bran β-glucan (Li et al. 2006). This structural variation may be studied by
181 "enzyme fingerprinting" (Ordaz-Ortiz and Saulnier, 2005), in which the polymers are digested
182 with specific enzymes (endoxylanase for AX, lichenase for β-glucan) and the structures and
183 proportions of the oligosaccharides which are released determines, by spectroscopic
184 imaging of sections, or by NMR spectrometry of hand dissected samples of tissue.

185 Barron et al. (2005) developed a protocol for comparing the structure of AX in the cell walls
186 of transverse sections of wheat grain, using sonication and washing with 70% ethanol to
187 remove the cell contents (notably starch) and protein adhering to the cell wall, and then
188 using FT-IR microspectroscopy to determine the structure of AX. Comparison of the spectra
189 with those of purified WE-AX and WU-AX allowed AX structures to be defined as highly
190 substituted with arabinose or less highly substituted. Figure 3 illustrates this approach, using
191 false colour to display the distributions of highly substituted AX (blue) in the centre of the
192 grain and less substituted AX (green) towards the periphery. However, it should be noted
193 these two structures were defined using an arbitrary cut off and are not discrete populations
194 of molecules. Similarly, there are gradients rather than discrete boundaries in the
195 distributions of this structural variation across the grain. Further application of this method
196 showed that the relative degree of arabinosylation varied between cultivars grown under the
197 same conditions (Toole et al., 2011), and that the structure changed during grain
198 development, with a decrease in the area of highly substituted AX and an increase in the
199 area of less substituted AX, a process referred to as "remodelling" (Toole et al., 2010).

200 FT-IR gives only limited information on AX structure and other approaches have been used
201 to provide more detailed information on variation in structure at the tissue level, including
202 Raman microspectroscopy which provides data on esterification with phenolic acids as well
203 as arabinosylation (Philippe et al, 2006; Toole et al., 2009), [1]NMR spectrometry to provide
204 more information on arabinosylation (Toole et al., 2010, 2011) and micro-scale enzyme
205 fingerprinting (as discussed above) (Saulnier et al., 2009).   These earlier studies have been
206 reviewed in detail by Saulnier et al. (2012).

207 More recently, Saulnier and colleagues have carried out enzyme hydrolysis directly on tissue
208 sections and identified the oligosaccharides released by MALDI mass spectroscopy imaging
209 (MSI) (Velickovik et al., 2014). In order to study spatial variation in structure they determined
210 four oligosaccharides: DP3 and DP4 fragments from β-glucan and AX5 and AX6 fragments
211 from AX. The latter have the structures XA_3XX and $XA_{2+3}XX$ and were selected as they are
212 known to be major contributors to variation in AX substitution. They showed that both AX
213 and β-glucan were concentrated in the outer cells of the endosperm in immature grain but
214 more evenly distributed throughout the endosperm at maturity. The ratio of AX5/AX6
215 fragments also confirmed other studies (discussed above) which showed lower
216 arabinosylation of AX in the outer layers. Similarly, the ratio of DP3/DP4 fragments released
217 from β-glucan was higher in the glucan-enriched outer cells of immature grain.

218   *2.4. Lipids.*

219 Lipids are minor components of the grain, accounting by weight for about 2.0-2.5% of flour
220 (Pareyt et al., 2011). They comprise many individual components (molecular species) which
221 are broadly classified into three types: polar lipids (phospholipids (PL) and galactolipids (GL)
222 which are structural components of membranes), triacylglycerols (TAG) (storage lipids) and
223 free fatty acids. However, there is great diversity within all three groups, notably in the head
224 groups of PLs and GLs and the fatty acids esterified to these components and TAGs. The
225 total lipid content of pearling fractions is greatest in those that contain the aleurone and
226 embryo and the lowest in fractions corresponding to the centre of the grain, with the
227 proportion of unsaturated fatty acids showing a similar pattern (Tosi et al., 2018). The
228 composition of molecular species also varies between pearling fractions, including the
229 contents of GLs (monogalactosyl diglyceride and digalactosyl diglyceride) (Gonzalez-
230 Thuillier et al, 2015).

231   **3. Linear gradients in the starchy endosperm**

232 Early reports of differences in the distribution of components in the wheat starchy
233 endosperm focused on radial gradients as these are readily observed in transverse sections
234 of grain. Consequently, analyses of pearling fractions were also largely interpreted in relation
235 to radial distribution. However, pearling actually removes more material from the ends of the
236 grains than from the central parts, resulting in an increasingly spherical shape (Fig 1).
237 Hence, the question must be asked whether gradients also exist along the longitudinal axis
238 of the grain. Although there is little work on this topic, two recent studies show that this is the
239 case.

240   *3.1.   Proteins.*

241 Shi et al (2019) determined longitudinal gradients in proteins by removing the embryos from
242 developing caryopses and then cutting them into three equal sections. The total gluten
243 protein content was lower in the section adjacent to the embryo, which may have related to
244 the presence in the dorsal part of modified starchy endosperm cells which support the
245 growth of the embryo. However, gradients in protein composition were also observed, with a
246 lower proportion of ⍵-gliadins (and higher proportions of other gluten proteins) in the
247 section adjacent to the embryo. The biological significance of this distribution is not known,
248 as there is no obvious relationship between ⍵-gliadins and embryo development.

249   3.2.   *Cell wall polysaccharides.*

250 Saulnier et al (2012) reviewed the current evidence for variation in cell wall polysaccharides
251 along the longitudinal axis of the grain. They reported that the starchy endosperm cells close
252 to the embryo (proximal to the point of attachment) were enriched in β-glucan, with AX being
253 highly substituted (with a ratio of A:X of about 0.7) in the same cells. The proportion of β-
254 glucan decreased towards the distal end of the grain, with lower AX substitution, although
255 the substitution was higher in prismatic cells than in central cells.

256 A more detailed study was reported by Fanuel et al. (2018), who analysed 30 consecutive
257 cross-sections of a mature grain using enzyme digestion to release oligosaccharides from β-
258 glucan and AX, which were then detected by MALDI MSI (as discussed above). Compilation
259 of the images allowed a 3D model of variation in polysaccharide structure to be constructed.
260 This confirmed that β-glucan was more abundant adjacent to the germ and in the central
261 starchy endosperm cells, while the AX was more highly substituted at the distal end of the
262 grain and around the crease.

263 Films made with highly substituted AX show higher water-diffusivity than those made with
264 low substituted AX (Ying et al, 2015) and Saulnier et al. (2012) suggested that structural
265 variation in AX may modulate the hydration properties of cell walls. Fanuel et al (2018)
266 therefore concluded that the distribution of highly substituted AX along the crease and
267 particularly in the vicinity of the germ, was consistent with the active transport of nutrients in
268 these regions

269   **4. Modulation of gradients by nutrition and environment**

270 He et al. (2013) compared the spatial patterns of gluten proteins and polymers in wheat
271 grain grown with two levels of nitrogen fertiliser, 100 kg Ha (which is typical of low input
272 farming systems in the UK) and 350 kg Ha (which is higher than used by UK farmers).
273 Nitrogen availability had the expected positive effect on total grain protein and on total gluten
274 proteins, but also affected the protein composition, with the proportions of ⍵-gliadins

275 increasing in all pearling fractions, and the proportion of HMW subunits increasing in all
276 fractions except the core. This differential effect of nitrogen is illustrated in Figure 4, which
277 shows gradients in the amounts of ⍵-gliadin protein and RNA transcripts in transverse
278 sections of grain grown at 100 and 350 kgN Ha (Wan et al., 2013).

279 Similar differential effects of N-supply on gluten protein composition in three longitudinal
280 sections were reported by Shi et al (2019), with increased proportions of ⍵-gliadins and
281 HMW subunits in all three sections at 21 and 28 days post anthesis. However, He et al
282 (2013) reported that there was little effect of nitrogen supply on the proportions of glutenin
283 polymers in the fractions, with the percentages of peaks F1 (comprising high molecular
284 weight polymers enriched in HMW subunits of glutenin) and F2 (comprising smaller
285 polymers enriched in LMW subunits of glutenin) being only marginally lower at 350 kg N Ha
286 and the ratio of %F1/%F2 being almost identical in grain grown at both nitrogen levels.

287 More detailed studies of factors determining gradients in protein amount were reported by
288 Savill et al. (2018) who developed an image analysis system to quantify the distribution of
289 protein in stained sections of developing grain. In addition to confirming previous studies of
290 protein distribution and the effects of nitrogen fertilisation, they also showed that the
291 gradients were enhanced by high temperatures post-anthesis. Zhong et al (2018) also
292 studied the effects of nitrogen fertilisation on protein distribution and processing quality,
293 showing that they could be modulated by the timing of application of top dressing.

294 Environmental effects on the remodelling of AX have also been reported, with the rate of
295 transition from highly arabinosylated to less arabinosylated AX being faster in grain grown at
296 higher temperature and limited water availability from 14 days after anthesis (Toole et al.,
297 2007). However, it is likely that this acceleration results from the increased rate of grain
298 maturation under these conditions rather than reprogramming of grain development.

5. Mechanisms determining the establishment of gradients during development of wheat grain

301 Microscopy of developing wheat grains using specific antibodies for immunolocalization
302 shows that the gradients in protein content and composition in the starchy endosperm are
303 established gradually during development, with different proteins accumulating at different
304 rates at different stages (Tosi et al., 2011). However, such analyses are only able to
305 measure protein accumulation, not protein deposition at a defined stage. In order to study
306 this, Moore et al (2016) fed ^{15}N-labelled glutamine to developing grains, via microcapillary
307 tubes inserted into the rachis, and determined protein deposition by measuring the degree of
308 enrichment of protein bodies in individual cells with ^{15}N using NanoSIMS (secondary ion
309 mass spectrometry). Isotope was fed for 6 hours and the developing caryopses harvested

310 either immediately, after 24 hours or after 7 days. This showed that the labelled substrate
311 was transported radially from its point of entry in the groove across the central starchy
312 endosperm to the protein-rich sub-aleurone cells. This is illustrated in Figure 5, which shows
313 that after 7 days most of the ^{15}N is present in large protein bodies in the sub-aleurone cells.

314 This raises the question of why the amino acid substrate is transported across the
315 developing starchy endosperm to be incorporated into protein in the cells just below the
316 aleurone layer. The simplest explanation is that the genes encoding gluten proteins are also
317 differentially expressed, being most strongly expressed in the sub-aleurone cells. This is
318 certainly the case for a LMW subunit gene, which is strongly expressed in these cells but
319 only weakly expressed in the central starchy endosperm (Stoger et al., 2001). Thus, high
320 levels of gluten protein gene expression may provide a sink for amino acid substrates in the
321 sub-aleurone cells, resulting in a concentration gradient which drives transport from the
322 transfer cells in the groove. This hypothesis is consistent with the study of Ugalde and
323 Jenner (1990) who measured the concentrations of soluble amino acids across the
324 developing endosperm. They found that the concentrations decreased from the endosperm
325 cavity to the mid-point and then increased from the midpoint to the periphery. Based on this
326 they concluded that the high level of protein accumulation in the peripheral cells could not be
327 attributed to the pattern of substrate supply and that the transport of amino acids did not limit
328 protein synthesis.

329 The difference in developmental programming of the sub-aleurone cells with respect to other
330 starchy endosperm cells may result from their different lineages, the sub-aleurone cells
331 being derived from anticlinal divisions of the aleurone cells, which continue to divide up to
332 about 14 days after anthesis (Bechtel and Wilson, 2003). This differential programming may
333 also account for the differences in the accumulation of starch between the sub-aleurone and
334 other starchy endosperm cells.

335 Whereas the gradients in protein composition may be explained, at least in part, by
336 differences in developmental programming due to cell lineages, the gradients in other
337 components are not as clear cut and the explanations may differ. In particular, Saulnier and
338 colleagues have suggested that variation in AX structure modulates the hydration and
339 permeability of cell walls and that variation in composition reflects the functional
340 requirements of the cells. Hence, in this case the gradients may reflect biological rather than
341 developmental differences between cell types.

342   **6. Is it possible to exploit spatial gradients in grain utilisation?**

343 The compositions of the fractions removed by pearling clearly reflect differences in the
344 spatial distributions of components within the grain that could have impacts on processing

10

345   quality. For example, the increased proportion of high molecular weight glutenin polymers in

346   the central part of the grain reported by He et al. (2013) implies that the central cells of the

347   starchy endosperm would have higher intrinsic quality for breadmaking, despite their lower

348   protein content. Similarly, the high content in galactolipids of the central core (Gonzalez-

349   Thuillier et al, 2015) may affect the breadmaking performance (Pareyt et al., 2011).

350   Differences in starch properties among pearling fractions (He et al., 2013; Zhou et al. 2018)

351   would also be expected to affect processing quality, and Zhou et al (2018) indeed reported

352   correlations with differences in quality for making bread and biscuits.

353   The question, therefore, is whether these gradients can be exploited by conventional milling

354   to produce flours with different compositions and end use properties. Milling is a highly

355   sophisticated process which has been developed to separate the starchy endosperm tissue

356   (white flour) from the outer layers (aleurone, pericarp and testa) and embryo (germ), which

357   together form the bran. Laboratory scale mills may produce up to 6 flour fractions, and

358   commercial mills over 20. In commercial milling, the purest flour fractions are recombined to

359   give white flour, with a total yield of between 78% and 80% of the grain weight.

360   However, the flour fractions are known to differ in composition. This difference in purity may

361   reflect their degree of contamination with bran. However, it may also reflect their origin in the

362   grain, with the purest streams coming from the central part of the starchy endosperm. It is

363   therefore of interest to determine how their compositions compare with those of pearling

364   fractions, so that mill streams can be more efficiently recombined to produce flours with

365   specific characteristics.

366   In order to answer this question Gonzalez-Thuillier et al. (2015) compared the lipid

367   compositions of pearling fractions with mill streams produced using a Buhler-MLU-202

368   laboratory mill, using the same grain sample. The mill generated 10 fractions comprising,

369   four bran fractions and six flour fractions, the latter representing three break fractions and

370   three reductions. Determination of the ash contents of these fractions indicated that Break 1

371   and Reduction 1 were the purest (0.3% ash), followed by Break 2 and Reduction 2 (0.4%)

372   and Break 3 and Reduction 3 (0.8 and 0.6%, respectively). Since the ash is derived from

373   contamination with bran, it is likely that fractions 1 correspond to the central starchy

374   endosperm and fractions 3 from the outer part. The range of variation in lipid composition

375   within the two sample sets was similar, but multivariate analysis of the two datasets showed

376   no clear correspondence between the fractions (Figure 6). Most of the pearling fractions

377   clustered together, with only the core clustering fairly close to the white flour fractions. It can

378   therefore be concluded that pearling can be used to identify differences in the spatial

379 distribution of components, but not to predict the compositions of fractions produced by roller
380 milling, which require instead direct analysis.

381 Nevertheless, this study, and other comparisons of the compositions of mill streams
382 (Prabhasankar et al., 2000; Nystrom et al., 2007; Ramseyer et al., 2011), suggest that
383 millers can indeed exploit differences in composition to produce specialist flours. For
384 example, flour fractions from the central starchy endosperm cells should give highly elastic
385 doughs suitable for breadmaking processes requiring high dough strength, such as the
386 Chorleywood Breadmaking Process, while fractions from the outer layers should give more
387 extensible doughs suitable for other products such as biscuits. Fractions from the outer
388 layers may also have sufficient extensibility and tenacity to be incorporated into pasta
389 making dough for fresh pasta or dry "special pasta". Finally, differences in
390 amylose:amylopectin ratio and in protein composition may also be exploited to improve the
391 "processability" of foods requiring frozen or chilled technology (such as chilled doughs,
392 bake–at-home breads and frozen cookie doughs), by increasing texture resilience.

393

394 **Acknowledgements.**

398 **References**

399 Andersson, A.A.M., Andersson, R., Piironen, V., Lampi, A.-M., Nystrom, L., Boros, D., Fras,
400 A., Gebruers, K., Courtin, C.M., Delcour, J.A., Rakszegi, M., Bedo, Z., Ward, J.L., Shewry,
401 P.R., Aman, P. 2013. Contents of dietary fibre components and their relation to associated
402 bioactive components in whole grain wheat samples from the HEALTHGRAIN diversity
403 screen. Food Chemistry 136, 1243-1248.

404 Barron, C., Parker, M.L., Mills, E.N.C., Rouau, X., Wilson, R.H. 2005. FTIR imaging of wheat
405 endosperm cell walls in situ reveals compositional and architectural heterogeneity related to
406 grain hardness. Planta 220, 667-677.

407 Barron, C., Surget, A., Rouau, X. 2007. Relative amounts of tissues in mature wheat
408 (*Triticum aestivum* L.) grain and their carbohydrate and phenolic acid composition. Journal of
409 Cereal Science 45, 88-96.

410 Bechtel, D.B., Wilson, J.D. 2003. Amylose development and starch granule development in
411 hard red winter wheat. Cereal Chemistry 80, 175-183Bechtel, D.B., Abecassis, J., Shewry,
412 P.R., Evers, T. 2009. The development, structure and mechanical properties of the wheat

413   grain. In: Khan, K. Shewry, P.R. (Eds.), Wheat: Chemistry and Technology, fourth ed.

414   American Association of Cereal Chemists, St Paul, pp. 51-95.

415   Bradbury, D., MacMasters, M., Cull, I.M. 1956. Structure of the mature wheat kernel. III.

416   Microscopic structure of the endosperm of hard red winter wheat. Cereal Chemistry 33, 361–

417   373.

418   Duffus, C. M., Murdoch, S.M. 1979. Variation in starch granule size distribution and amylose

419   content during wheat endosperm development. Cereal Chemistry 56, 427-429.

420   Evers, T., Millar, S. 2002. Cereal Grain Structure and Development: Some Implications for

421   Quality. Journal of Cereal Science 261, 32-84.

422   Fanuel, M., Ropartz, D., Guillon, F., Saulnier, L., Rogniaux, H. 2018. Distribution of cell wall

423   hemicelluloses in the wheat grain endosperm: a 3D perspective. Planta 248, 1505-1513

424   González-Thuillier, I., Salt, L., Chope, G., Penson, S., Skeggs, P., Tosi, P., Ward, J., Wilde,

425   P., Shewry, P., Haslam, R. 2015. Distribution of lipids in the wheat grain determined by

426   analysis of milling and pearling fractions. Journal of Agricultural and Food Chemistry 63,

427   10705-10716.

428   He, J., Penson, S., Powers, S., Hawes, C., Shewry, P.R., Tosi, P. 2013. Spatial patterns of

429   gluten protein and polymer distribution in wheat grain. Journal of Agricultural and Food

430   Chemistry 61, 6207-6215.

431   Kent, N.L. 1966. Subaleurone endosperm cells of high protein content. Cereal Chemistry 43,

432   585-601.

433   Kent, N.L., Evers, A.D. 1969. Variation in protein composition within the endosperm of hard

434   wheat. Cereal Chemistry 46, 293-300.

435   Li, W., Cui, S. W., Kakuda, Y. 2006. Extraction, fractionation, structural and physical

436   characterization of wheat β-D-glucans. Carbohydrate Polymers, 63, 408-416.

437   Millet, M.O., Montembault, A., Autran, J.C. 1991. Hordein compositional differences in

438   various anatomical regions of the kernel between two different barley types. Sciences des

439   Alimentations 11, 155-161.

440   Moore, K.L., Tosi, P., Palmer, R., Hawkesford, M.J., Grovenor, C.R.M., Shewry, P.R. 2016.

441   The dynamics of protein body formation in developing wheat. Plant Biotechnology Journal 9,

442   1876-82.

443   Morel, M.-H., Dehlon, P., Autran, J. C., Leygue, J. P., BarL'Helgouac'h, C. 2000. Effects of

444   temperature, sonication time, and power settings on size distribution and extractability of

445   total wheat flour proteins as determined by size-exclusion high-performance liquid

446   chromatography. Cereal Chemistry 77:685-691.

447   Nyström, L., Paasonen, A., Lampi, A.-M., Piironen, V. 2007. Total plant sterols, steryl

448   ferulates and steryl glycosides in milling fractions of wheat and rye. Journal of Cereal

449   Science 45, 106-115.Ordaz-Ortiz, J.J., Devaux, M.-F., Saulnier, L. (2005) Classification of

450 wheat varieties based on structural features of arabinoxylans as revealed by endoxylanase
451 treatment of flour and grain. Journal of Agricultural and Food Chemistry 53, 8349-8356.

452 Pareyt, B., Finnie, S. M., Putseys J. A., Delcour. J. A. 2011. Lipids in bread making: sources,
453 interactions, and impact on bread quality. Journal of Cereal Science 54, 266-279.

454 Phillipe, S., Barron, C., Robert, P., Devaux M.-F., Saulnier, L., Guillon, F. 2006.
455 Characterization using Raman microspectroscopy of arabinoxylans in the walls of different
456 cell types during the development of wheat endosperm. Journal of Agricultural and Food
457 Chemistry 54, 5113-5119.

458 Prabhasankar, P., Sudha, M.L., Haridas R, P. 2000. Quality characteristics of wheat flour
459 milled streams. Food Research International 33, 381-386.

460 Ramseyer, D.D., Bettge, A.D., Morris, C.F. 2011. Distribution of total, water-unextractable,
461 and water-extractable arabinoxylans in wheat flour mill streams. Cereal Chemistry 88, 209-
462 216.

463 Saris, W.H., Asp, N.G., Björck, I., Blaak, E., Bornet, F., Brouns, F., Frayn, K.N., Fürst, P.,
464 Riccardi, G.,

465 Saulnier, L., Guillon, F., Chateigner-Boutin, A.-L. 2012. Cell wall deposition and metabolism
466 in wheat grain. Journal of Cereal Science 56, 91-108

467 Saulnier, L., Robert, P., Grintchenko, M., Jamme, F., Bouchet, B. Guillon, F. 2009. Wheat
468 endosperm cell walls: Spatial heterogeneity of polysaccharide structure and composition
469 using micro-scale enzymatic fingerprinting and FT-IR microspectroscopy. Journal of Cereal
470 Science 50, 312-317

471 Savill, G., Michalski, A., Powers, S.J., Wan, Y., Tosi, P., Buchner, P., Hawkesford, M.J.
472 2018. Temperature and nitrogen supply Interact to determine protein distribution gradients in
473 the wheat grain endosperm. Journal of Experimental Botany 69, 3117-3126.

474 Shewry, P.R., Halford, N.G., Tatham, A.S., Popineau, Y., Lafiandra, D., Belton, P. 2003. The
475 high molecular weight subunits of wheat glutenin and their role in determining wheat
476 processing properties. Advances in Food and Nutrition Research 45, 221-302.

477 Shi, Z., Wang, Y., Wan, Y., Hassall, K., Jiang, D., Shewry, P.R., Hawkesford, M.J. 2019.
478 Gradients of Gluten Proteins and Free Amino Acids along the Longitudinal Axis of the
479 Developing Caryopsis of Bread Wheat. Journal of Agricultural and Food Chemistry 67, 8706-
480 8714.

481 Shinde, S. V., Nelson, J. E., Huber, K. C. 2003. Soft wheat starch pasting behavior in
482 relation to A- and B-type granule content and composition. Cereal Chemistry, 80, 91-98.

483 Stone, B., Morell, M.K., 2009. Carbohydrates. In: Khan, K., Shewry, P.R. (Eds.), Wheat:
484 Chemistry and Technology, 4th ed. American Association of Cereal Chemists, St Paul, MN,
485 pp. 299-362.

486 Stoger E, Parker M, Christou P, Casey R. 2001. Pea legumin overexpressed in wheat
487 endosperm assembles into an ordered paracrystalline matrix. Plant Physiology 125, 1732–
488 1742.

489 Tomlinson, K., Denyer, K. 2003. Starch synthesis in cereals. Advances in Botanical
490 Research including Advances in Plant Pathology 40, 1-61.

491 Toole, G.A., Wilson, R.H., Parker, M.L., Wellner, N.K., Wheeler, T.R., Shewry, P.R., Mills,
492 E.N.C. 2007. The effect of environment on endosperm cell wall development in *Triticum*
493 *aestivum* during grain filling: an infrared spectroscopic imaging study. Planta 225, 1393–
494 1403.

495 Toole, G.A., Barron, C., Le Gall, G., Colquhoun, I.J., Shewry, P.R., Mills, E.N.C. 2009.
496 Remodelling of arabinoxylan in wheat (*Triticum aestivum*) endosperm cell walls during grain
497 filling. Planta 229, 667-680.

498 Toole. G.A., Le Gall, G., Colquhoun, I.J, Johnson, P., Bedö, Saulnier, L., Shewry, P.R., Mills,
499 E.N.C. 2011. Spectroscopic analysis of diversity in arabinoxylan structures in endosperm cell
500 walls of wheat cultivars (*Triticum aestivum*) in the HEALTHGRAIN diversity collection.
501 Journal of Agricultural and Food Chemistry 99, 7075-7082

502 Toole. G.A., Le Gall, G., Colquhoun, I.J., Nemeth, C., Saulnier, L., Lovegrove, A., Pellny, T.,
503 Velickovic, D., Ropartz, D., Guillon, F., Saulnier, L., Rogniaux, H. 2014. New insights into the
504 structural and spatial variability of cell-wall polysaccharides during wheat grain development,
505 as revealed through MALDI mass spectroscopy imaging. Journal of Experimental Botany 65,
506 2079-2091.

507 Wilkinson, M.D., Freeman, J., Mitchell, R.A.C., Mills, E.N.C., Shewry, P.R. 2010. Temporal
508 and spatial changes in cell wall composition in developing grains of wheat cv. Hereward.
509 Planta 232, 677-689.

510 Toole, G.A., Wilson, R.H., Parker, M.L., Wellner, N.K., Wheeler, T.R., Shewry, P.R., Mills,
511 E.N.C. 2007. The effect of environment on endosperm cell-wall development in *Triticum*
512 *aestivum* during grain filling: an infrared spectroscopic imaging study. Planta 225, 1393-
513 1403.

514 Tosi, P., He, J., Lovegrove, A., Gonzalez-Thuillier, I., Penson, S., Shewry, P.R. 2018.
515 Gradients in compositions in the starchy endosperm of wheat have implications for milling
516 and processing. Trends in Food Science and Technology 82, 1-7.

517 Tosi, P., Parker, M., Gritsch, C.S., Carzinaga, R., Martin, B., Shewry, P.R. 2009. Trafficking
518 of storage proteins in developing grain of wheat. Journal of Experimental Botany, 60, 979-
519 991.

520 Tosi, P., Gritsch, C.S., He, J., Shewry, P.R. 2011. Distribution of gluten proteins in bread
521 wheat (*Triticum aestivum*) grain. Annals of Botany 108, 23-25.

522 Ugalde, T. D., Jenner, C. F. 1990. Substrate Gradients and regional patterns of dry matter

523 deposition within developing wheat endosperm. II. Amino acids and protein. Australian

524 Journal of Plant Physiology 17, 395-406.

525 Wan, Y., Gritsch, C.S., Hawkesford, M.J., Shewry, P.R. 2013. Effects of nitrogen nutrition on

526 the synthesis and deposition of the ω-gliadins of wheat. Annals of Botany 113, 607-615

527 Zhong, Y., Yang, M., Cai, J., Wang, Z., Zhou, Q., Cao, W., Dai, T, Jiang, D. 2018. Nitrogen

528 topdressing timing influences the spatial distribution patterns of protein components and

529 quality traits of flours from different pearling fractions of wheat (*Triticum aestivum* L.) grains.

530 Field Crops Research 216, 120-128

531 Zhou, Q., Li, X., Yang, J., Zhou, L., Cai, J., Wang, X., Dai, T., Cao, W., Jiang, D. 2018.

532 Spatial distribution patterns of protein and starch in wheat grain affect baking quality of bread

533 and biscuit. Journal of Cereal Science 79, 362-369.

534 Ying, R.F., Saulnier, L., Bouchet, B., Barron, C., Ji, S.J. Rondeau-Mouro, C. 2015. Multiscale

535 characterisation of arabinoxylan and beta-glucan composite films. Carbohydrate Polymers

536 122, 248-254.

537

538 **Figure legends**

539 **Figure 1.** Cross section of a developing grain of durum wheat cv Ofanto at 20 days DPA,

540 stained with toluidine blue to show the distribution of protein (taken from Tosi et al., 2009

541 and 2018).

542 The left hand image shows the whole grain with the areas in boxes A and B expanded in the

543 central and right hand images, respectively. The bar in the cross-section represents 1mm,

544 the bars in panels 1 and 2 100μm. Note the high concentration of protein in the sub-aleurone

545 cells in area B.

546 **Figure 2.** Pearling of grain of wheat cv Hereward.

547 Part A shows the pearling mill; part B the whole grain and the cores after a typical

548 experiment of 6 pearling cycles; part C the cumulative removal of material from the grain

549 over 6 cycles using a single grain sample.

550 **Figure 3.** Spectroscopic FT-IR image overlaid onto a light microscope image of a transverse

551 section of a grain of wheat cv. Spark at 30 DPA.

552 The grain section has been treated to remove the cell contents allowing the spectra of the

553 cell walls to be determined. Previous studies had established that the height of a shoulder in

554 the FT-IR spectrum at 1,075 cm-1 reflects the extent of substitution of the AX structure

555 (Toole et al. 2007; 2009). A colour was therefore assigned to each pixel depending on the

556 height of the shoulder at 1,075 cm-1 compared to that of the major peak at 1,041 cm-1. If the

557 shoulder was below 66% the pixel was coloured green to represent low substituted AX and if

558 it was above 66% it was coloured blue to represent highly substituted AX. White represents

559 remaining starch, and black represents holes or pixels where the amount of AX was too low

560 to determine. Figure kindly provided by Dr. Geraldine Toole (IFR, Norwich, UK).

561

562 **Figure 4.** Spatial patterns of deposition of total proteins and ω-gliadins in the starchy

563 endosperm of wheat cv Hereward grown at nitrogen levels of 100kg/ha (left panel: A, C, E,

564 G) and 350 kg/ha (right panel: B, D, F, H).

565 A-B, sections at 27 DPA stained for protein bodies with Naphthol Blue Black; E-F, *in situ*

566 hybridisation of transcripts related to ω2-gliadins (C,D) and ω5-gliadins (E,F) at 17 DPA; G-

567 H, immunolocalisation of ω5-gliadin at 27 DPA; The immunofluorescence labelling in G and

568 H is displayed in false yellow colour. Scale bars: 500μm (A-H). Taken from Wan et al (2013).

569

570 **Figure 5.** Graphical representation of the size and ^{15}N enrichment of protein bodies along a

571 transect of starchy endosperm tissue (from the nucellar projection to the aleurone layer) after

572 labelling at 20 DPA and imaging after either 24 hours (A) or 7 days (B), showing transport of

573 ^{15}N glutamine substrate across the developing starchy endosperm.

574 Individual protein bodies are displayed as "bubbles", which correspond in size to their

575 measured areas. The positions of the protein bodies correspond to their locations along the

576 transect (x axis) and their degree of enrichment with ^{15}N (y axis). Sections were washed to

577 remove free ^{15}N glutamine

578 Taken from Moore et al (2016).
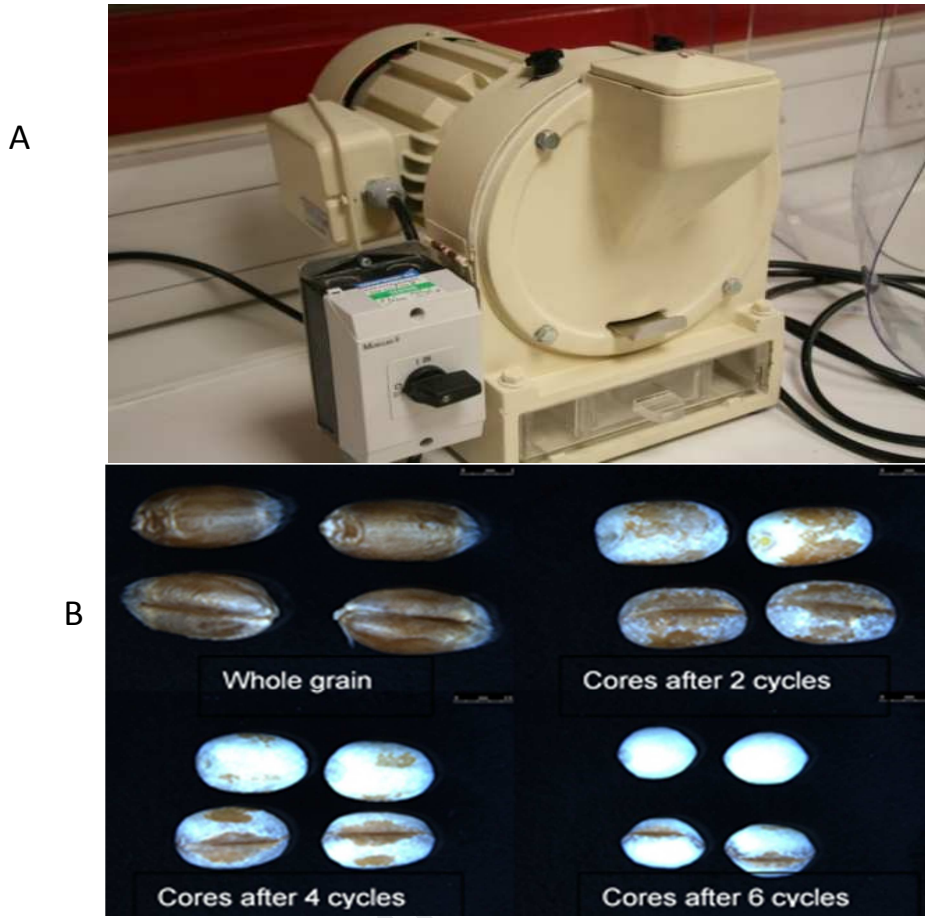
579

580 **Figure 6.** Principal Component Analysis (PCA) fractions from milling and pearling of wheat
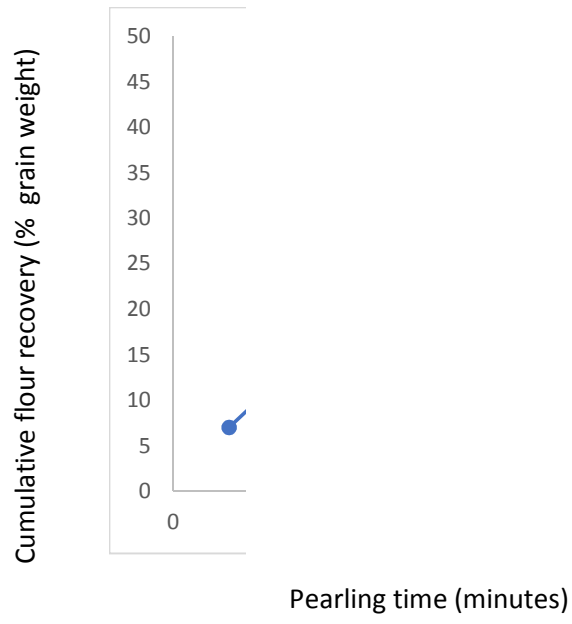
581 cv Hereward

582 A: PCA scores plot showing PC1 (40 %) vs PC2 (18 %). Pearling fractions: PF1, pearling

583 fraction 1; PF2, pearling fraction 2; PF3, pearling fraction 3; PF4, pearling fraction 4; PF5,

584 pearling fraction 5; PF6, pearling fraction 6 and core. Milling fractions: B1, break 1; R1,

585 reduction 1; B2, break 2; R2, reduction 2; B3, break 3; R3, break 3; OF, offal fraction; O-OT,

586 offal over-tail; BF, bran fraction; B-OT, bran over-tail.

587 B: PCA loadings plot of PC1 vs PC2 showing the molecular species responsible for the

588 separation in A. Variables are coloured according to their lipid class and are labelled

589 according to chain length and double bond number. Lipid classes are diacylglycerol (DAG),

590 digalactosyl diglyceride (DGD), free fatty acids (FFA), lysophosphatidyl choline (LPC),

591 monogalactosyl diglyceride (MGD), phosphatidyl choline (PC), phosphatidyl ethanolamine

592 (PE), phosphatidyl glycerol (PG), phosphatidyl inositol (PI), and triacylglycerol (TAG). ,

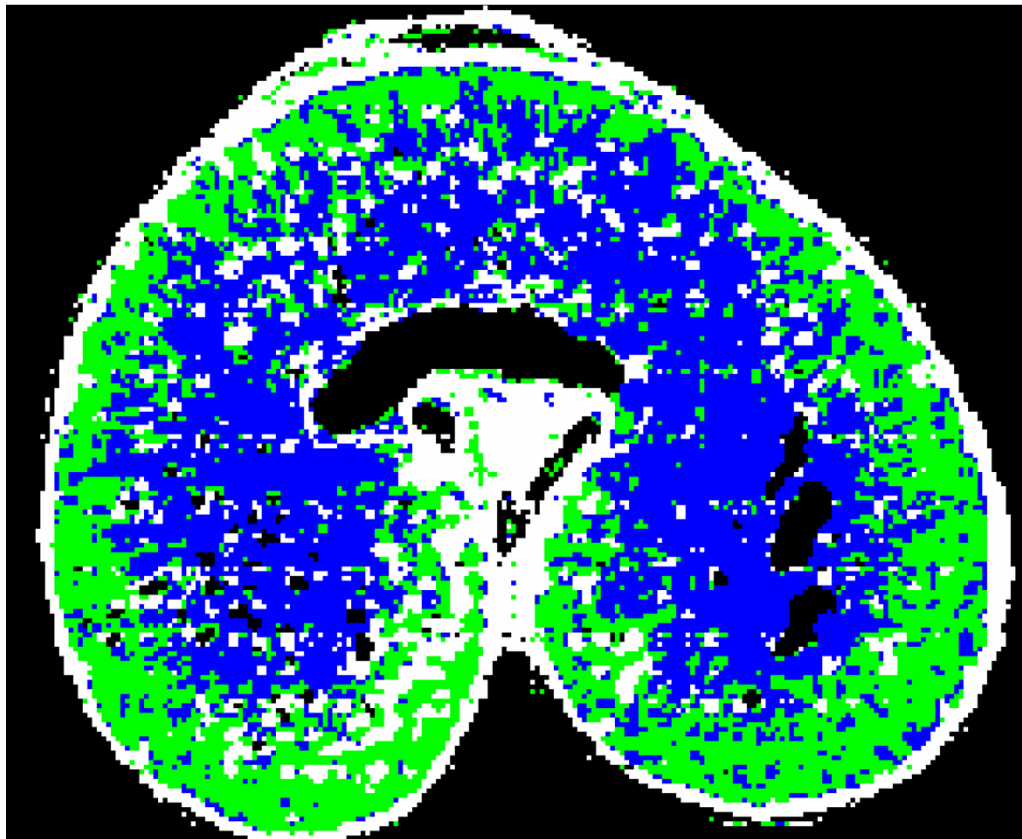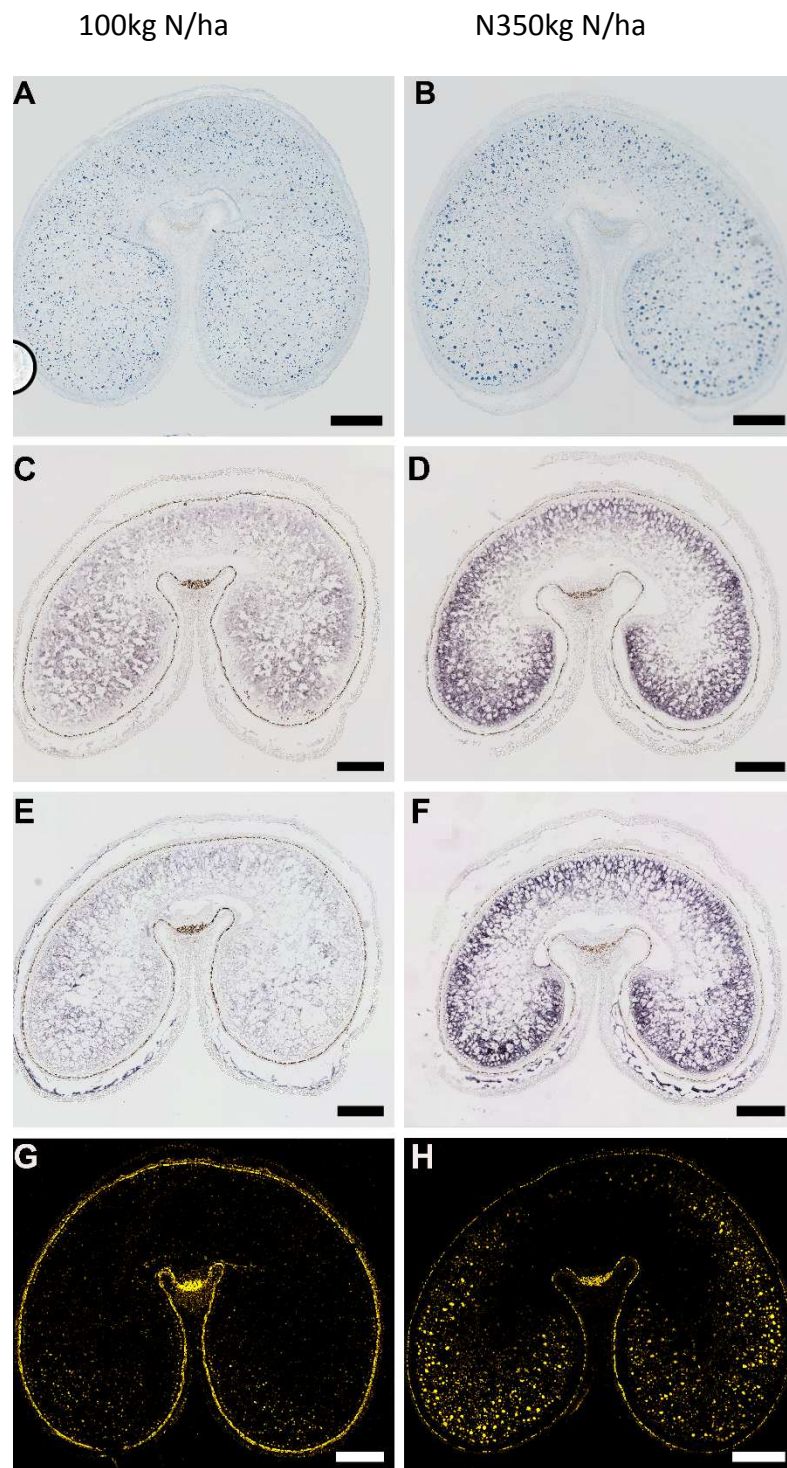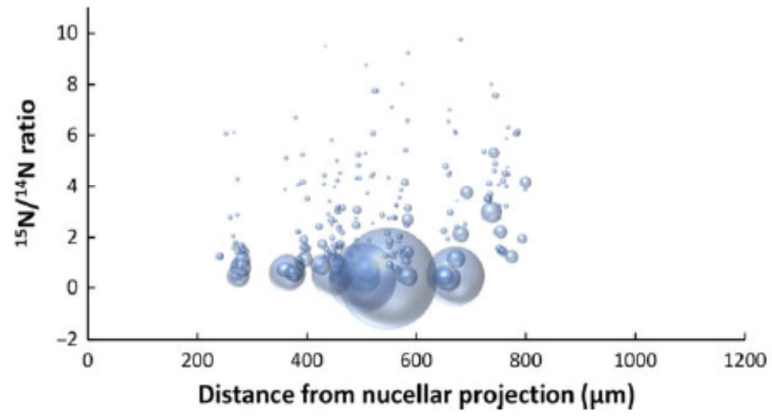593 Taken from Gonzalez-Thuillier et al. (2015).

Figure 2

A

B

Whole grain

Cores after 2 cycles

Cores after 4 cycles

Cores after 6 cycles

C

Cumulative flour recovery (% grain weight)

Pearling time (minutes)
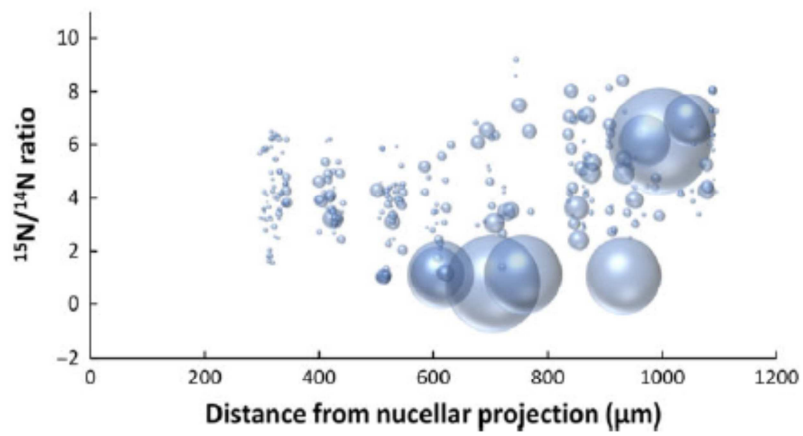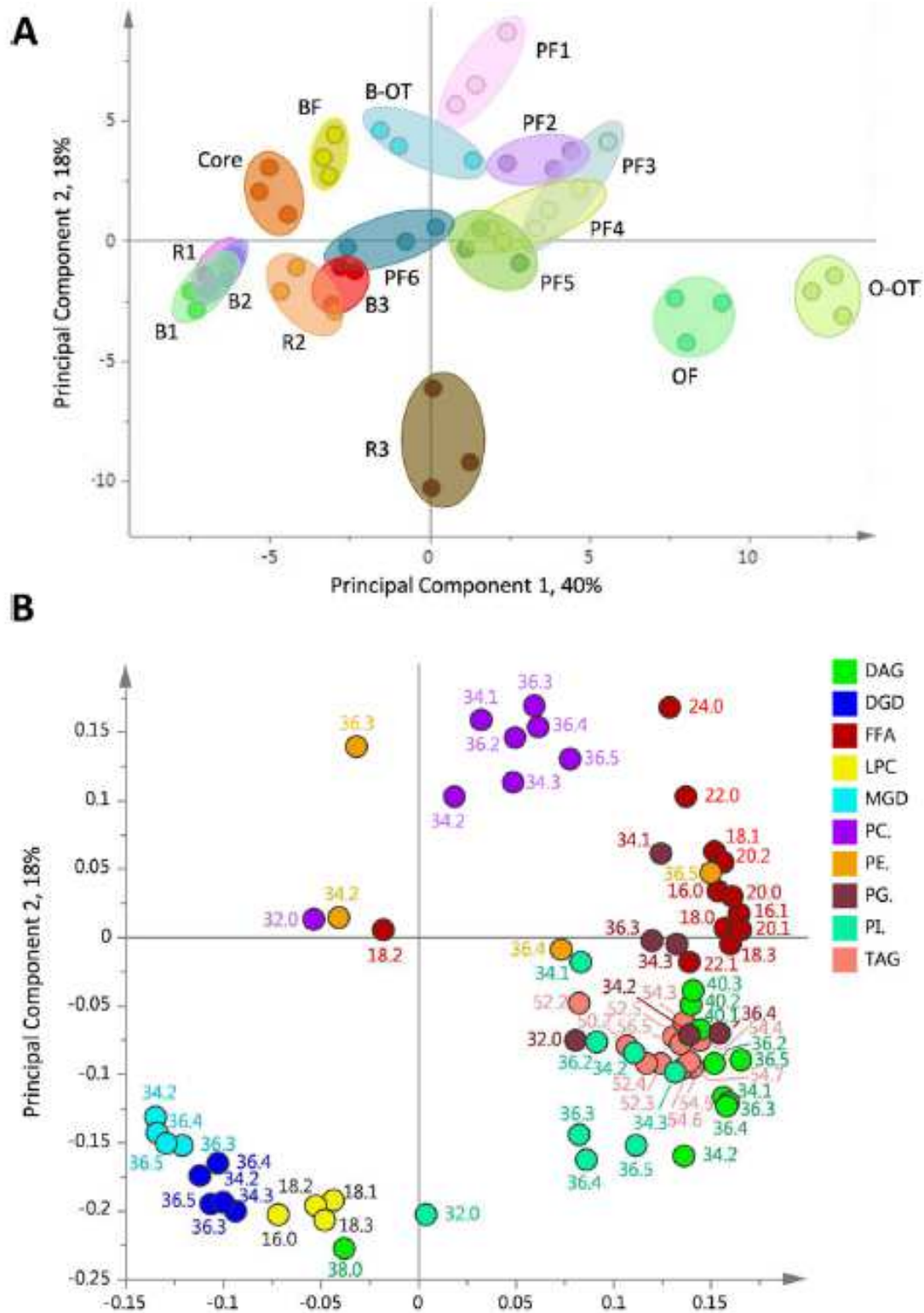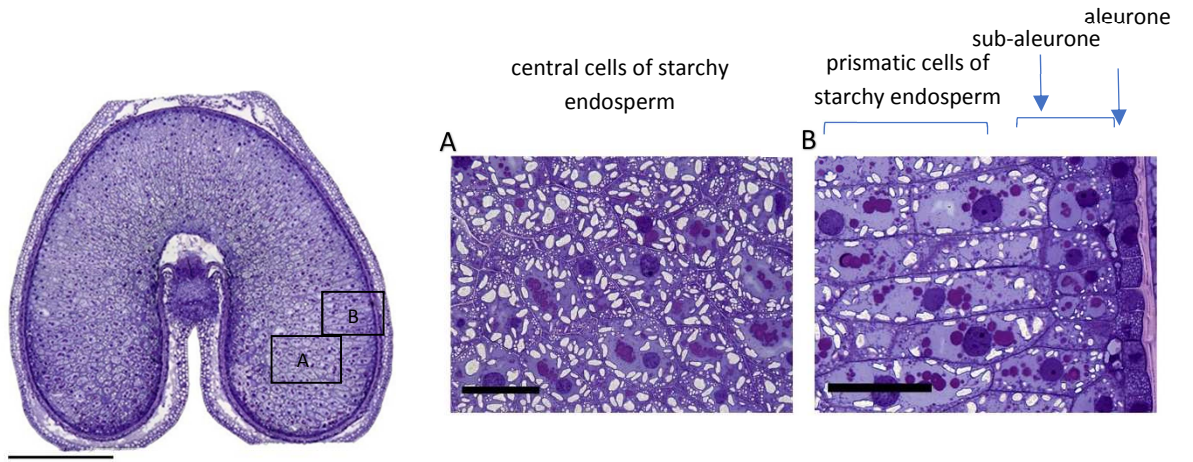
Figure 3

Figure 4

100kg N/ha   N350kg N/ha

Figure 5

A

B

Figure 6

- The mature starchy endosperm of wheat comprises three cell types
- These differ in their contents of functional components
- These differences are reflected in the compositions of mill streams
- These differences may affect functionality
- Hence innovative milling can be used to prepare flours for special uses

Declaration of interest statement

The authors have no competing interests